Journal of Marine Research, 67, 71–88, 2009

On the interannual variability of nitrogen fixation in the subtropical gyres

by Fanny M. Monteiro[1,2] and Michael J. Follows[1]

ABSTRACT

Time-series observations of geochemical tracers and diazotroph abundances in the northern subtropical gyres suggest variability in nitrogen fixation on interannual and longer timescales. Using a highly idealized model of the biogeochemistry and ecology of a subtropical gyre, we explore the previously proposed hypothesis that such variability is regulated by an internal "biogeochemical oscillator." We find, in certain parameter regimes, self-sustained oscillations in nitrogen fixation, community structure and biogeochemical cycles even with perfectly steady physical forcing. During the oscillations of nitrogen fixation, "blooms" of diazotrophs occur at intervals between a year and several decades, consistent with the observed variability. The period of the oscillations is strongly regulated by the exchange rate between the thermocline and mixed-layer waters. The oscillatory solutions occur in a relatively small region of parameter space, but one in which the relative fitness of diazotrophs and non-diazotrophs are closely matched and the time-averaged biomass of each class of phytoplankton is maximized.

1. Introduction: Decoupling of ocean nitrogen and phosphorus cycles

The nitrogen and phosphorus cycles are globally tightly coupled in the ocean. They are dominated by the biological consumption of dissolved inorganic forms in the mixed layer, the export of organic forms to depth and subsequent remineralization. They are subject to common physical transport processes, riverine and atmospheric sources (Benitez-Nelson, 2000; Gruber, 2004), and burial in sediments. Redfield (1934) noted that these common processes lead to a tight relationship between the dissolved inorganic nitrogen and phosphorus (DIN and DIP) and the stoichiometry of bulk organic matter in the global ocean. Recently, emphasis has been placed on understanding the decoupling of nitrogen and phosphorus due to the more rapid oceanic turnover of nitrogen by nitrogen fixation and denitrification (Fanning, 1992; Gruber and Sarmiento, 1997). Nitrogen fixation in the ocean is largely performed by a variety of diazotrophic phytoplankton in the pelagic ocean including colonial cyanobacteria, unicellular cyanobacteria (Zehr *et al.*, 2001), as well as some endosymbiotic diazotrophs observed in diatoms (Carpenter *et al.*, 1999). A great deal of

1. Department of Earth, Atmospheric and Planetary Sciences, Massachusetts Institute of Technology, Cambridge, Massachusetts, 02139, U.S.A.
2. Corresponding author. ***email: fmonteir@mit.edu***

the current understanding of marine diazotrophy has been revealed through the study of the large colonial cyanobacteria *Trichodesmium* which is mostly abundant in oligotrophic tropical and subtropical waters (Carpenter and Romans, 1991; Capone *et al.*, 1997), and is perhaps the most significant oceanic diazotroph (Karl *et al.*, 2002). *Trichodesmium* have relatively slow growth rate, high elemental N:P ratio and high iron demand (LaRoche and Breitbarth, 2005; Masotti *et al.*, 2007). These characteristics reflect the additional requirements for the production of nitrogenase and the reduction of dinitrogen gas (Tyrrell, 1999; Klausmeier *et al.*, 2004). Recent observations suggest similar characteristics for unicellular diazotrophs (Falcón *et al.*, 2005; Goebel *et al.*, 2008).

Along with seasonal variations, nitrogen fixation has been observed to change on interannual and decadal timescales. Steven and Glombitza (1972) measured interannual variability of *Trichodesmium* abundance in the vicinity of Barbados for a 3-year period. The other evidences come from indirect tracers, such as N* (Michaels *et al.*, 1996; Gruber and Sarmiento, 1997; Deutsch *et al.*, 2001) and $\mathrm{DIN}_{xs} = \mathrm{NO}_3^- - R^{Phy}\mathrm{PO}_4^{3-}$ (Hansell *et al.*, 2004; Bates and Hansell, 2004), where N* differs only by a constant offset. These tracers measure variations in inorganic N:P relative to the Redfield ratio, $R^{Phy} = 16$ (Redfield *et al.*, 1963; Ho *et al.*, 2003; Quigg *et al.*, 2003). Increasing values of these tracers following water parcel trajectories are interpreted to reflect diazotrophic activity. They have been used to assess integrated nitrogen fixation rates in the subtropical North Atlantic (Gruber and Sarmiento, 1997; Hansell *et al.*, 2004). Conversely, decreasing values following water parcels are interpreted as signatures of denitrification.

In extremely oligotrophic regions, phytoplankton may also satisfy their resource requirements by utilizing dissolved organic forms of nitrogen (DON) (Karl *et al.*, 1997; Zehr and Ward, 2002; Berman and Bronk, 2003; Varela *et al.*, 2005) and phosphorus (DOP) (Björkman *et al.*, 2000; Björkman and Karl, 2003). DOP utilization has also been noted in *Trichodesmium* (Karl *et al.*, 2002; Sohm and Capone, 2006). Hence it might be more appropriate to include the organic forms in the metric of the relative abundance of biologically available nitrogen and phosphorus. We consider an analog of DIN_{xs}

$$\mathrm{TDN}_{xs} = \mathrm{TDN} - R^{Phy}\mathrm{TDP} \tag{1}$$

where TDN and TDP are total dissolved nitrogen and phosphorus (this corresponds to the proN* tracer proposed by Dennis Hansell and Nick Bates; personal communication; see also Landolfi *et al.*, 2008). TDN_{xs} measures the excess of nitrogen for the total dissolved pools. Here we consider $\mathrm{TDN}_{xs} = 0$ as the transition point between nitrogen and phosphorus limitation in the case where phytoplankton have Redfieldian elemental ratios and may consume dissolved both inorganic and organic forms.

Observations in the subtropical oceans, at the Hawaii Ocean Time-series (HOT; Karl, 2002) and Bermuda Atlantic Time-series Study (BATS; Bates and Hansell, 2004) sites, provide an unparalleled view of the temporal variation in local N-P decoupling. Both reveal interannual to decadal variations of TDN_{xs} and/or DIN_{xs}. Here we focus on interpreting the observations at HOT (Fig. 1). There, TDN_{xs} decreases monotonically with depth. Negative

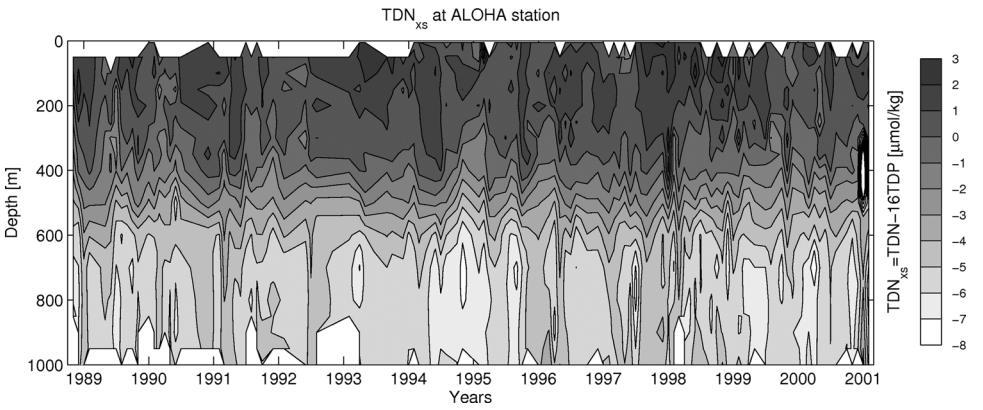

Figure 1. Time-series of the profile of TDN_{xs} (http://hahana.soest.hawaii.edu/ hot/hot_jgofs.html). The observations are averaged for each month and interpolated linearly with depth.

values in the thermocline ($<-4\ \mu mol\ kg^{-1}$) reflect the regional influence of denitrification in the oxygen minimum zone (500 to 1500 m; Gruber and Sarmiento, 1997; Deutsch *et al.*, 2001). TDN_{xs} exhibits strong temporal variability, swinging between positive and negative values in the upper ocean with an amplitude of more than 1 $\mu mol\ kg^{-1}$. This suggests a flip-flop between phosphorus and nitrogen limitation ($TDN_{xs} > 0$ and $TDN_{xs} < 0$ respectively) and, perhaps, nitrogen fixation (Karl *et al.*, 1997; Karl, 2002). Interannual variability is also evident in the DIN_{xs} record of the North Atlantic (Bates and Hansell, 2004) and the mechanisms discussed here may also be relevant in that basin.

Suggested mechanistic explanations for these interannual changes include physical forcing related to large-scale climate variability, based on comparisons between ENSO and NAO indices and upper ocean DIN_{xs} and TDN_{xs} (Karl *et al.*, 1995, 1997; Bates and Hansell, 2004). Changes in atmospheric forcing can affect mixed-layer stratification and the aeolian deposition of iron: a more stratified upper ocean may favor oligotrophy, high light conditions, and thus *Trichodesmium* growth and nitrogen fixation (LaRoche and Breitbarth, 2005). An increase in aeolian iron deposition may alleviate iron stress imposed by the high demand of diazotrophs (Sanudo-Wilhelmy *et al.*, 2001).

Karl (2002) suggested an alternative explanation for the variability. He hypothesized an internal ocean "diazotroph oscillator" in which nitrogen limitation in the surface waters stimulates nitrogen fixation and an export of nitrogen-rich organic detritus. The excess nitrogen accumulates in the thermocline and is eventually brought to the surface by winter entrainment. This drives the mixed layer to phosphorus limitation. Diazotrophy is suppressed, TDN_{xs} declines and surface waters return to a nitrogen-limited regime.

Here we demonstrate that such an internal oscillation is possible in an idealized numerical model of the nitrogen and phosphorus cycles in subtropical gyres (Section 2). We will show that, even in the absence of variable external forcing, such a system can sustain a "diazotroph

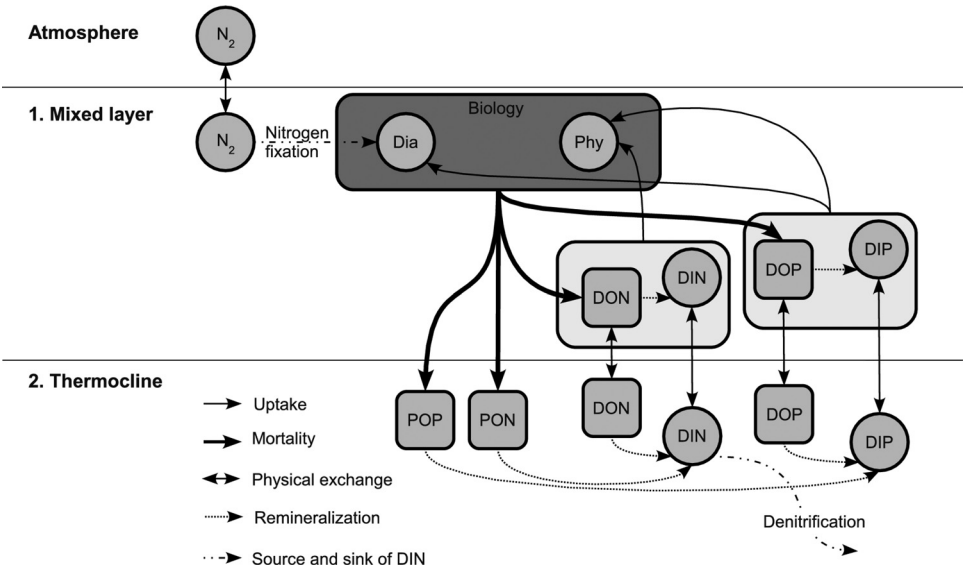

Figure 2. Schematic diagram of the two-layer model. DIN and DIP represent inorganic fixed nitrogen and phosphorus. DON and DOP are the dissolved organic forms. *Dia* are diazotrophs and *Phy* are non-diazotrophic phytoplankton. Here *Dia* are assumed to fix all of their nitrogen requirement. *Dia* and *Phy* can utilize both dissolved inorganic and dissolved organic forms of nutrients.

oscillator" leading to a periodic nitrogen fixation (Section 3). We will use the model to elucidate how the relative fitness of the model phytoplankton relates to environmental conditions and show how the timescale of the oscillations depends strongly on the rate of ventilation of thermocline waters (Section 4).

2. A model of subtropical nitrogen and phosphorus cycles

We employ a highly idealized, two-layer representation of the N and P cycles in a subtropical gyre (Fig. 2). The layers reflect a surface mixed layer (order 100 m thick) and a permanent thermocline (order 1000 m thick), which annually exchange a volume comparable to the integrated Ekman pumping and the seasonal deepening (entrainment) of the mixed layer (Williams, 2001). We choose not to represent any variability of the physical environment, keeping the model simple in order to explore the internal variability of the system. We explicitly represent the transport and biological transformations of DIN, DIP (dissolved inorganic N and P), DON, DOP (dissolved organic N and P), PON and POP (particulate organic N and P). We measure biomass using phosphorus as the currency since it is globally conserved in the model though either resource could be used for this purpose. The full prognostic equations and model parameter ranges are listed in Tables 1, 2 and 3. We resolve two broad functional classes of phytoplankton: diazotrophs (*Dia*) and all other phytoplankton (*Phy*), using parameterizations that have much in common with the

Table 1. Surface layer prognostic equations. Here pp represents primary production by *Phy* (non-diazotroph phytoplankton) and dp is primary production by *Dia* (diazotrophs). μ^{Phy} and μ^{Dia} (d^{-1}) are the maximum specific growth rates of *Phy* and *Dia*. Maximum growth rates are modulated by the availability of inorganic and organic forms of the limiting nutrient; either TDN = DIN + DON or TDP = DIP+DOP. $\Gamma_N = DIN_1/TDN_1$ and $\Gamma_P = DIP_1/TDP_1$ are the relative abundances of each form. f_{DOM} is a factor representing a reduction of growth rate, assuming an additional energetic cost for utilizing organic substrates. K_N and K_P are the half saturation coefficients for N and P and K_N is defined as $16K_P$ such that, in oligotrophic conditions, *Phy* are limited by P availability when $TDN_1 > 16TDP_1$, and by N when $TDN_1 < 16TDP_1$. Loss due to grazing and mortality is parameterized by a highly simplified linear mortality with rate coefficients M^{Phy} and M^{Dia}.

$$\frac{dPhy}{dt} = \underbrace{pp}_{\text{Primary production}} - \underbrace{M^{Phy}Phy}_{\text{Grazing + Mortality}} \tag{4}$$

$$\frac{dDia}{dt} = dp - M^{Dia}Dia \tag{5}$$

$$\frac{dDIP_1}{dt} = \underbrace{-\frac{V}{z_1}(DIP_1 - DIP_2)}_{\text{Physical transport}} - \underbrace{\Gamma_P(pp + dp)}_{\text{Total uptake of } DIP_1} + \underbrace{\lambda DOP_1}_{\text{Remineralization}} \tag{6}$$

$$\frac{dDIN_1}{dt} = -\frac{V}{z_1}(DIN_1 - DIN_2) - \Gamma_N R^{Phy} pp + \lambda DON_1 \tag{7}$$

$$\frac{dDOP_1}{dt} = -\frac{V}{z_1}(DOP_1 - DOP_2) - (1 - \Gamma_P)(pp + dp) \tag{8}$$

$$+(1 - S)(M^{Phy}Phy + M^{Dia}Dia) - \lambda DOP_1 \tag{9}$$

$$\frac{dDON_1}{dt} = -\frac{V}{z_1}(DON_1 - DON_2) - (1 - \Gamma_N)R^{Phy} pp \tag{10}$$

$$+(1 - S)(R^{Phy}M^{Phy}Phy + R^{Dia}M^{Dia}Dia) - \lambda DON_1 \tag{11}$$

$$pp = \mu^{Phy}(\Gamma + f_{DOM}(1 - \Gamma))min\left\{\frac{TDP_1}{TDP_1+K_P}; \frac{TDN_1}{TDN_1+K_N}\right\} Phy \tag{12}$$

$$dp = \mu^{Dia}(\Gamma_P + f_{DOM}(1 - \Gamma_P))\frac{TDP_1}{TDP_1+K_P} Dia \tag{13}$$

Table 2. Thermocline prognostic equations. R_{rest} is the TDN_{xs} towards which the thermocline is restored in a simple parameterization of denitrification. τ_{rest} is the restoring time scale.

$$\frac{dDOP_2}{dt} = -\frac{V}{z_2}(DOP_2 - DOP_1) - \lambda DOP_2 \tag{14}$$

$$\frac{dDON_2}{dt} = -\frac{V}{z_2}(DON_2 - DON_1) - \lambda DON_2 \tag{15}$$

$$\frac{dPOP}{dt} = \frac{z_1}{z_2}S(M^{Phy}Phy + M^{Dia}Dia) - \lambda POP \tag{16}$$

$$\frac{dPON}{dt} = \frac{z_1}{z_2}S(R_{Phy}M^{Phy}Phy + R_{Dia}M^{Dia}Dia) - \lambda PON \tag{17}$$

$$\frac{dDIP_2}{dt} = -\frac{V}{z_2}(DIP_2 - DIP_1) + \lambda(DOP_2 + POP) \tag{18}$$

$$\frac{dDIN_2}{dt} = -\frac{V}{z_2}(DIN_2 - DIN_1) + R_{Phy}\lambda(DON_2 + PON)$$

$$\underbrace{-\frac{1}{\tau_{rest}}(DIN_2 - 16DIP_2 - R_{rest})}_{\text{Restoring term}} \tag{19}$$

Table 3. Parameter values of the control case (Fig. 3). The right column presents the range of measured parameter values from the literature which is explored in sensitivity studies. τ_{rest} is the timescale with which thermocline DIN_{xs} is restored towards the target value, reflecting the vigor of denitrification and import of N-depleted waters. The values for the diazotrophic parameters are all based on *Trichodesmium* data. *(a)* for annual maximum depth in subtropical gyres (Boyer-Montegut *et al.*, 2004); *(b)* for North Pacific subtropical gyre (Qiu and Huang, 1995), whereas the North Atlantic subtropical gyre: 50−150 m yr^{-1} (Marshall *et al.*, 1993); *(c)* Tyrrell (1999); Dutkiewicz *et al.* (2001); Fennel *et al.* (2002); *(d)* for *Trichodesmium* (LaRoche and Breitbarth, 2005); *(e)* Capone *et al.* (1997); *(f)* Redfield *et al.* (1963); Ho *et al.* (2003); Quigg *et al.* (2003); *(g)* Klausmeier *et al.* (2004); *(h)* Libes (1992). The initial conditions used in the model are: $Phy = 10^{-2}$, $Dia = 10^{-3}$, $DIP_1 = 0.1$, $DIN_1 = 0.05$, $DIP_2 = 1$, $DIN_2 = 15$, $DOP_1 = 0.20$, $DON_1 = 5$, $DOP_2 = 0.1$, $DON_2 = 4$, $POP = PON = 0$ (μmolP kg^{-1} for *Phy* and *Dia* otherwise μmol kg^{-1}).

Symbol	Name	Control Run/Unit	Literature (Range)
z_1	Mixed layer depth	100 m	50–200[a]
z_2	Permanent thermocline depth	1000 m	
V	Ventilation rate	30 m yr^{-1}	5–50[b]
μ^{Phy}	Non-diazotroph phytoplankton maximum growth rate	1 d^{-1}	0.1–4[c]
μ^{Dia}	Diazotroph maximum growth rate	0.20 d^{-1}	$<\mu_{Phy}$[c], 0.12–0.32[d]
f_{DOM}	Reducing factor for organic uptake compare to inorganic uptake	0.4 no unit	<1
K_P	Phosphate half saturation constant	0.005 μmolP kg^{-1}	0.0015–0.05[c]
K_N	Fixed nitrogen half saturation constant	0.08 μmolN kg^{-1}	$16 \times K_P$
M^{Phy}	Non-diazotroph grazing - mortality rate	0.6 d^{-1}	0.05–1.2[c]
M^{Dia}	Diazotroph grazing - mortality rate	0.5 d^{-1}	$<M^e_{Phy}$
R^{Phy}	N:P Redfield ratio	16 no unit	16
R^{Dia}	Diazotroph N:P ratio	60 no unit	$>R^{e,g}_{Phy}$, 16–125[d]
S	POM fraction	0.4 no unit	<0.5[h]
λ	Remineralization rate	0.006 d^{-1}	0.006–0.15[c]
R_{rest}	Restored thermocline TDN_{xs}	−6 no unit	∼local mean
τ_{rest}	Restoring time scale	2 yr	2–10

previously published models of Tyrrell (1999) and Fennel *et al.* (2002). Non-diazotrophic phytoplankton are assumed to have a Redfieldian elemental ratio (R^{Phy} = N:P = 16:1; Table 3), and diazotrophs a fixed N:P ratio of 60 (LaRoche and Breitbarth, 2005). *Dia* and *Phy* are constrained to occur only in the surface layer (Fig. 2) in a simple representation of light limitation. Nutrient-limited growth of both functional types is represented by a Michaelis-Menten relationship (Dugdale, 1967) with a smaller maximum specific growth rate (μ in d^{-1}) for *Dia*, due to the high energetic cost of nitrogen fixation. This is consistent with observed growth rates (Tables 1 and 3). Both organism types are subject to phosphorus limitation. As for nitrogen, we assume that *Dia* acquires all of its nitrogen by fixation, while *Phy* may also be limited by the availability of dissolved N, following Liebig's law of the minimum. Here, we also allow both phytoplankton types to consume DOP and/or DON

when the inorganic equivalent forms are in limiting concentration. Growth is thus limited by the availability of total dissolved P or N (TDP or TDN; Table 1, Eqs. 12 and 13). We assume that utilization of the organic form is energetically more expensive for phytoplankton, in the idea that phytoplankton invest more machinery into photoautotrophy. This should make them more likely to use inorganic than organic nutrients. We impose an arbitrary 60% decrease in maximum growth rate (f_{DOM}) when using organic forms for both autotroph classes. We also impose that inorganic and organic nutrients are utilized in proportion to their relative abundance (e.g. $\Gamma_P = \mathrm{DIP}/(\mathrm{DIP} + \mathrm{DOP})$). In this idealized study we do not explicitly represent a dynamic iron cycle but focus instead on N and P dynamics as the possible driver of a internal "diazotroph oscillator". Iron limitation by a constant environmental concentration could be considered as folded into the differential of maximum growth rates of *Phy* and *Dia*.

In this idealized framework, grazing and mortality of *Phy* and *Dia* are represented as simple linear loss terms (Eqs. 4 and 5). We impose a reduced mortality for *Dia* since *Trichodesmium* have been observed to have fewer predators (Capone *et al.*, 1997). Detritus is partitioned into a dissolved and particulate organic matter pools (DOM and POM) in fixed fraction S (Libes, 1992). POM is assumed to sink rapidly and to be completely remineralized in the thermocline, while DOM is transported by the vertical mixing (ventilation) and may be remineralized in either the mixed layer or the thermocline. We parameterize denitrification simply, restoring DIN so as to drive DIN_{xs} toward a prescribed value in the thermocline (Eq. 19), reflecting either local denitrification or mixing with waters denitrified elsewhere in the ocean. Phosphorus is thus conserved over the whole domain. Nitrogen is not; its dynamic budget is determined by the balance between nitrogen fixation and the parameterized denitrification. We initialize the model with plausible values of the prognostic variables, and integrate it forward in time for several hundred years until a statistically steady state is reached.

3. Model results: A diazotroph oscillator

We explore the model's behavior over a plausible range of biogeochemical parameter values, guided by observations and laboratory measurements (see the Literature (Range) column in Table 3). In much of the explored parameter space, the model reveals perfectly steady solutions in which both diazotrophs and other phytoplankton co-exist (Fig. 3). This follows the ecological theory for co-existence, since two resources or "limiting factors" are present in the modeled environment (Armstrong and McGehee, 1980). In the illustrated example, diazotrophs persist with considerably lower biomass than the other phytoplankton (0.5×10^{-3} μmolP kg^{-1} and 3×10^{-3} μmolP kg^{-1} for diazotrophs and other phytoplankton respectively). These modeled concentrations compare favorably (given the highly idealized nature of the system) with the general character of the observed concentrations at HOT, which vary between 0.3 and 1.3 $\times 10^{-3}$ μmolP kg^{-1} for diazotrophs (Karl *et al.*, 1997; Fennel *et al.*, 2002), and 7 and 20 $\times 10^{-3}$ μmolP kg^{-1} for the total phytoplankton population

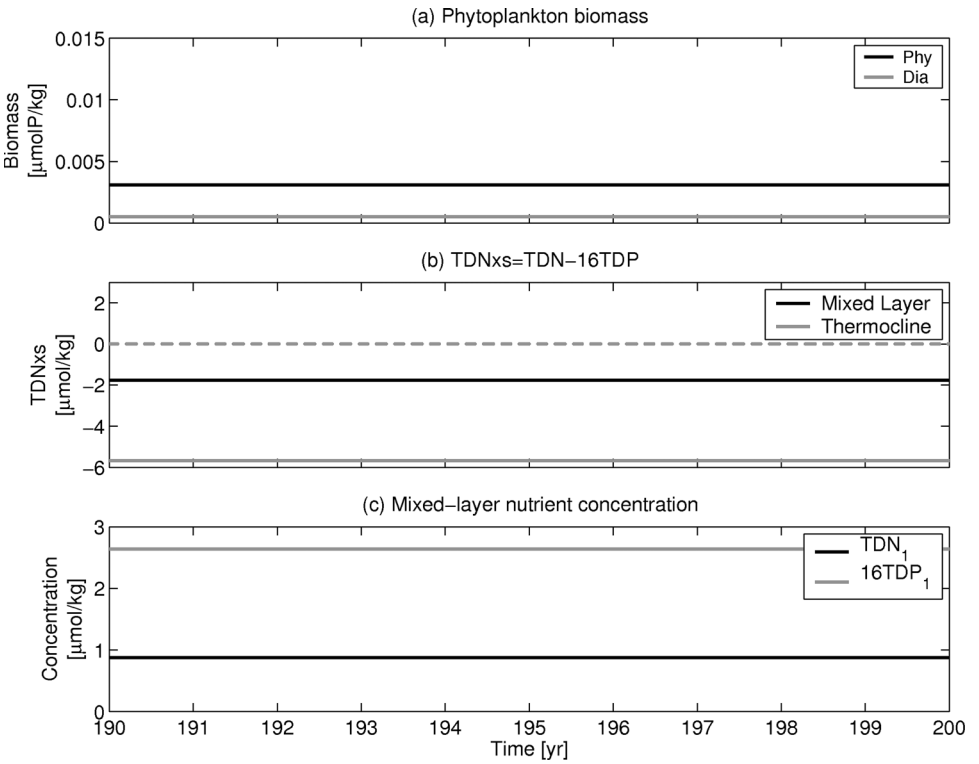

Figure 3. Example steady solution in a configuration with ventilation rate and thermocline DIN_{xs} set appropriate for the North Pacific subtropical gyre. (a) Biomass of diazotrophs (*Dia*) and non-diazotrophic phytoplankton (*Phy*); (b) TDN_{xs} in the mixed layer and thermocline; (c) TDN and 16×TDP in the mixed layer. All units are in µmolP kg^{-1}. Model parameter values are given in Table 3.

(Karl *et al.*, 2001)[3]. In these non-oscillatory model regimes interannual variations of nitrogen fixation must be forced externally in response to changes in the physical environment, for example.

Nevertheless, in some regions of the explored parameter space, the model exhibits oscillatory solutions supporting the notion of a self-sustained diazotroph oscillator (Karl, 2002). In these regimes, the abundances of diazotrophs and other phytoplankton vary in regular cycles, with period ranging from a year or two to several decades (e.g. Fig. 4). The oscillations occur in the absence of any externally imposed physical or biogeochemical variability. Figure 4 illustrates an example relevant to the North Pacific subtropical gyre, with ventilation rate of about 30 m yr^{-1} and a relatively strong sink of nitrogen in the thermocline (2 year restoration timescale for thermocline DIN_{xs}; Table 3). The illustrated solution has a period

3. Assuming a P:Chl ratio of 0.10 µmolP kg^{-1} (mg Chl m^{-3})$^{-1}$ (Fasham *et al.*, 1990).

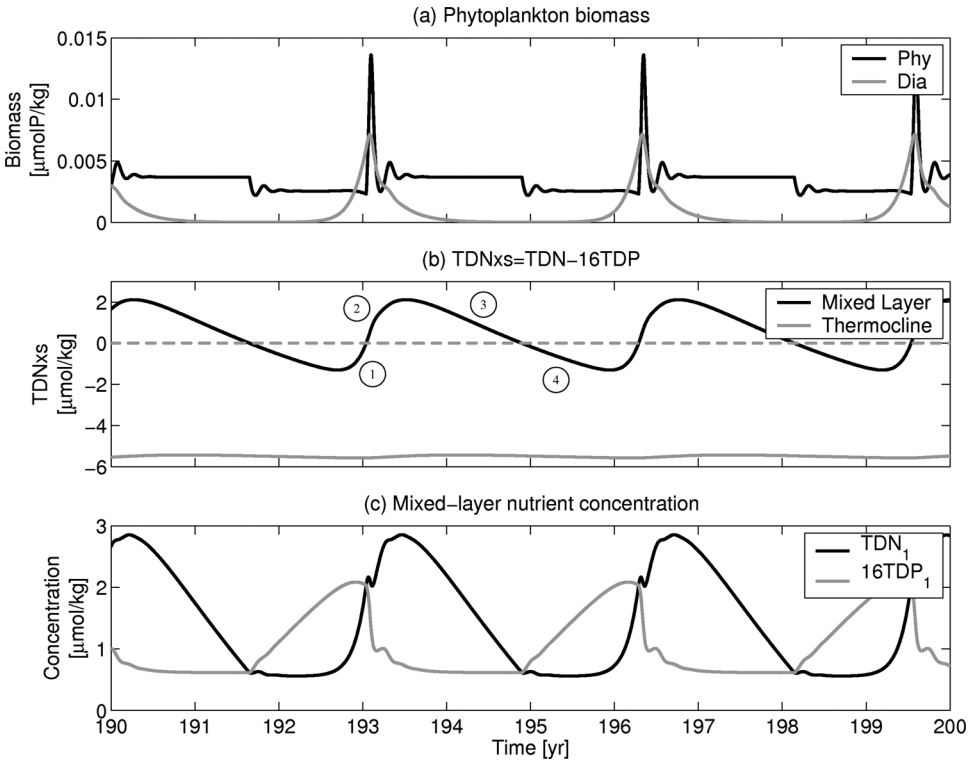

Figure 4. Example oscillatory solution in a configuration with ventilation rate and thermocline DIN_{xs} set appropriate for the North Pacific subtropical gyre (see Table 3). (a) Biomass of diazotrophs (*Dia*) and non-diazotrophic phytoplankton (*Phy*); (b) TDN_{xs} in the mixed layer and thermocline. The inset numbers represent the different steps of the "diazotroph oscillator" and are recalled in the schematic of the oscillator in Figure 5; (c) TDN and 16×TDP in the mixed layer. Physical forcing and all parameter values are constant. Time variation is the result of an internal "biogeochemical oscillator".

of 3.5 years, not inconsistent with the character of the interannual variability observed at HOT (see section 1 and Fig. 1). The order of magnitude of the modeled phytoplankton abundance is broadly in agreement with the HOT observations ($Dia \sim 1 \times 10^{-3}$ μmolP kg^{-1} and $Phy \sim 3 \times 10^{-3}$ μmolP kg^{-1}). Such a highly idealized system can never precisely capture such a complex real system in all details. Modeled TDN_{xs} concentrations also vary over a range consistent with the observations: between −1.3 to 2.1 μmol kg^{-1}. The modeled nitrogen fixation rate, $\sim 25 \times 10^{-2}$ molN m^{-2} yr^{-1}, is somewhat larger than observed in the vicinity of Hawaii, ($3.1-5.1 \times 10^{-2}$ molN m^{-2} yr^{-1} ; Karl *et al.*, 1997), but is sensitive to the assumed N:P ratio of the diazotrophs and the accessibility of organic phosphorus. It also reflects the very crude vertical resolution of the model where nitrogen fixation occurs throughout the mixed layer with a fixed 100 m thickness. We also see a diazotroph oscillator in solutions with parameter values more appropriate to the North Atlantic subtropical gyre:

faster subduction rates (V ~50−150 m yr^{-1}) and a weaker influence of denitrification in the thermocline (τ_{rest} ~5–10 yr).

a. Mechanism of the diazotroph oscillator

The model's diazotroph oscillator switches between a nitrogen limited regime (Fig. 4; $TDN_{xs} < 0$, phases 1 and 4) and a phosphorus limited regime ($TDN_{xs} > 0$, phases 2 and 3). In the nitrogen limited regime (Fig. 4; phase 1), where only non-diazotrophs are nitrogen limited, diazotrophs are competitive and their population increases. This "blooming" of diazotrophs creates relatively nitrogen-rich organic matter in the mixed layer. Since export ratios are low in the oligotrophic oceans, much of this organic material is remineralized in the surface ocean increasing mixed layer TDN_{xs} (Figs. 4b and 4c, phases 1 and 2) and driving surface waters to phosphorus limitation. Diazotrophs are no longer competitive because of their relatively slow growth rate and their population declines again to very low abundance (Figs. 4a and 4b, phase 2). Subsequently, dilution by denitrified thermocline waters draws down the TDN_{xs} of the mixed layer back to a nitrogen limited regime (Fig. 5).

The mechanism of the model's oscillator is broadly consistent with that hypothesized by Karl (2002) but differs in some details. Since most organic matter is remineralized close to the surface and denitrification occurs at depth, in the model entrainment of thermocline waters represents a sink of surface TDN_{xs}, rather than a source. The extent to which this is the case depends upon the bio-availability of the dissolved organic nitrogen pool which is assumed to be fully available in the model for simplicity.

b. What regulates the period of the oscillation?

The TDN_{xs} record at Hawaii indicates variability of nitrogen fixation on timescales of a few years (Karl, 2002). Evidence for "regime shifts" in this region are also suggestive of decadal variations (Karl *et al.*, 2001). Sensitivity studies with the numerical model over the range of biogeochemical parameter values (Table 3) reveal oscillatory solutions with periods between ~1 and ~30 years. In the model, the phase of increasing diazotroph population and surface TDN_{xs} is relatively rapid (Figs. 4 and 5). The period is largely determined by the rate at which mixed-layer TDN_{xs} (TDN_{xs1}) declines back towards a nitrogen limited regime (phases 3 and 4). Assuming negligible concentration of *Dia* and a linear decline of TDN_{xs1} (details in the Appendix), we can approximate the rate of change in TDN_{xs1} as a function of the mixing with thermocline TDN_{xs} (TDN_{xs2}): $dTDN_{xs1}/dt \approx (V/z_1)TDN_{xs2}$ (Fig. 4b). We estimate the time interval, Δt, over which the system returns to nitrogen limited conditions, i.e. the approximate period of the oscillation:

$$\Delta t \sim \frac{z_1}{V}\frac{\Delta TDN_{xs1}}{TDN_{xs2}} \tag{2}$$

where ΔTDN_{xs1} is the amplitude (μmol kg^{-1}) of the changes in mixed-layer TDN_{xs}. The timescale is inversely related to the ventilation rate, V, the rate of exchange of denitrified

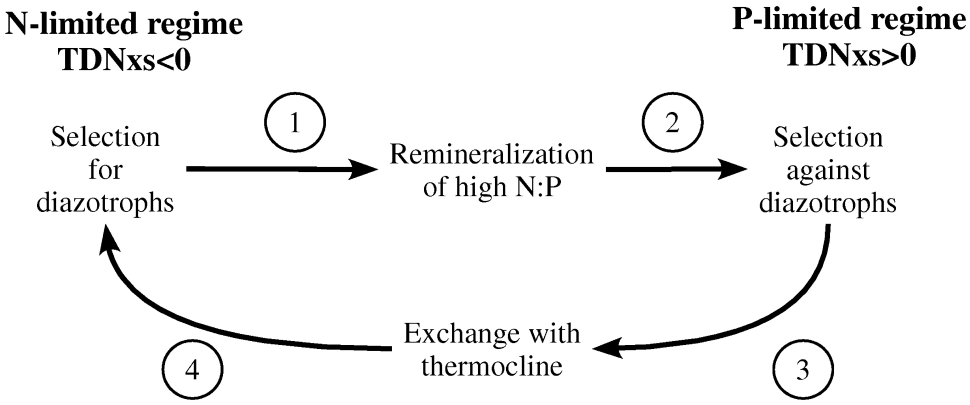

Figure 5. Mechanism of the diazotroph oscillator. Numbers correspond to the phases of the cycle as indicated in Figure 4b.

waters between thermocline and mixed layer. The simple scaling solution accurately predicts relationship of the model's oscillation period to the ventilation rate (Fig. 6). The range of ventilation rates span typical values for the subtropical North Pacific (5−50 m yr^{-1}; Qiu and Huang, 1995) and subtropical North Atlantic (50−150 m yr^{-1}; Marshall *et al.*, 1993).

Sensitivity studies also show that the amplitude of the oscillations increases with the "fitness" of diazotrophs relative to the other phytoplankton, as measured by μ/M, the ratio of their maximum growth and mortality rates (Section 4).

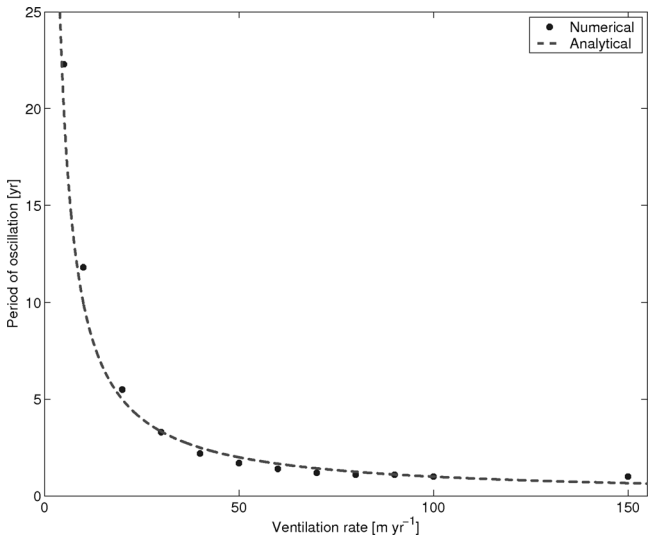

Figure 6. Period of the oscillations as a function of the ventilation rate (V). The dots represent numerical solutions and the dashed line the best fit for the scaling solution (Eq. 2).

4. Ecological regimes in the model

The numerical model supports the hypothesis that a diazotroph oscillator could drive (at least some of) the observed interannual and longer timescale changes in ecosystem structure and nitrogen fixation in the subtropical gyres (Karl *et al.*, 2001). On the other hand, this behavior is only evident in certain parameter regimes. Under what circumstances do oscillatory solutions occur?

We examine a suite of tens of integrations, covering a broad region of parameter space, to tease out further insight into the viability of the diazotroph oscillator in this particular system. We examine the model solutions in the context of the relative fitness of *Dia* and *Phy*, here measured by the ratio of maximum growth rate and mortality: $(\mu/M)^{Dia}$ and $(\mu/M)^{Phy}$ (Fig. 7). Each plotted point represents a single solution of the model. Three broad regimes are evident: non-oscillatory solutions with co-existing non-diazotrophs and diazotrophs (diamonds), non-oscillatory solutions where diazotrophs exclude the other phytoplankton (crosses), and oscillatory solutions where both functional types co-exist (circles). Each regime occupies a clearly defined region in the μ/M space (sketched and annotated in Fig. 7b).

In the regime where $(\mu/M)^{Dia} < (\mu/M)^{Phy}$ the relatively low mortality of diazotrophs is outweighed by their slow maximum growth rate (Fig. 7a, diamonds). Nitrogen and phosphorus are both potentially limiting and co-existence is supported. In this idealized model, both organism classes are assigned the same half-saturation for phosphorus uptake, K_P, and both are assumed able to utilize either organic or inorganic phosphorus. When TDP/(TDP $+ K_P$), a measure of the degree of phosphorus limitation, approaches 1 phosphorus is no

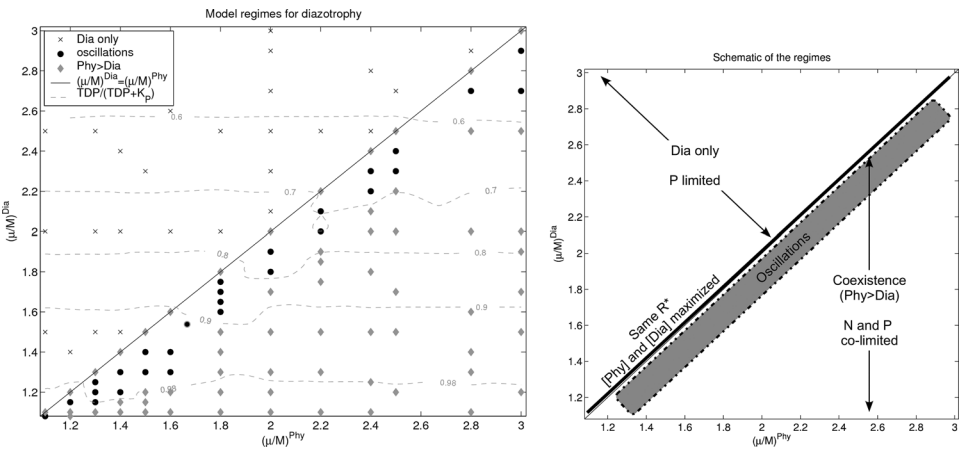

Figure 7. Regimes of the model solution as a function of μ/M, the ratios of maximum growth rate and mortality of *Dia* and *Phy*. (a) Plotted points indicate model parameters from a single integration. Black circles – oscillatory solution; gray diamonds – steady solution, *Dia* < *Phy*; crosses – steady solution, *Dia* only. Contours of environmental phosphorus stress, TDP/(TDP + K_P), are also shown as gray, dashed lines. (b) Schematic of the model regimes.

longer limiting and, as long as the environmental N:P ratio is not too far from Redfield, growth may no longer be significantly limited by the availability of macro-nutrients. In this situation, where the diazotrophs low maximum growth rate more than compensates for their reduced mortality their abundance becomes very low, though they are never completely excluded.

When $(\mu/M)^{Dia} > (\mu/M)^{Phy}$, the model diazotrophs exclude other phytoplankton. Here, the relatively fit diazotrophs thrive and the remineralization of the nitrogen-rich organic detritus derived from them relieves nitrogen limitation. In this regime, where phosphorus is the single limiting resource, diazotrophs exclude the other phytoplankton. The slow growth rate of *Trichodesmium* in laboratory cultures suggests that this situation, if at all plausible, would have to be due to low mortality and weakened top down control. Observations suggest that diazotrophs do not typically dominate the phytoplankton population in terms of biomass except, perhaps, in very local bloom conditions.

Oscillatory solutions occur in a small region close to the line where $(\mu/M)^{Dia} = (\mu/M)^{Phy}$ (Fig. 7), but within the region where non-diazotrophs are fitter. Assuming steady state for both phytoplankton (Eqs. 4 and 5), we may infer the TDP concentration at which each population could maintain an equilibrium

$$\mathrm{TDP} \approx \frac{K_P}{\frac{\mu^i}{M^i} - 1}, \tag{3}$$

where i is either *Dia* or *Phy*. This concentration is equivalent to the "R*" of resource competition theory (Tilman, 1977). In a perfectly steady, single-resource environment, the organism type with the lowest R* should exclude all others (Stewart and Levin, 1973). Since *Phy* and *Dia* have the same K_P, the continuous line of equal μ/M is where both organisms have the same R*, i.e. each could exist at equilibrium. Hence the oscillatory solutions with co-existence occur when the two organism classes are characterized by very similar R* values. They are closely matched in terms of this measure of fitness. It is interesting to note that the time-averaged biomass of both *Phy* and *Dia* are maximized along the line where Phy and Dia fitnesses are equal. This maximization of biomass and productivity is right on top of the oscillatory solutions.

That the oscillatory solutions occur in a very narrow region of parameter space may suggest that this situation should be considered unlikely to occur in reality. On the other hand, this special region of parameter space, makes evolutionary sense: in an oligotrophic environment photo-autotrophs must evolve towards the low R* of their fit competitors if they are not to be excluded. It is also the region where biomass and primary productivity are maximized. Perhaps then, this narrow region of parameter space where the biogeochemical oscillator also reflects an evolutionary stable state for the ocean's subtropical gyres. However, more studies are needed at this point to fully understand the reason why the oscillator is located in such a region of the parameter space.

5. Summary and discussion

We have developed an idealized model of the nitrogen and phosphorus cycles and ecosystem of subtropical gyres. We have explored the possibility that an internal biogeochemical oscillator might exist in the subtropical gyres, giving rise to some of the observed interannual to decadal variability in surface water biogeochemistry and ecology near Hawaii (Karl *et al.*, 2001; Karl, 2002).

Though highly simplified, the model can capture some of the character of the diazotrophic and non-diazotrophic populations and surface water biogeochemistry in the northern subtropical gyres. Of course, such a highly idealized model cannot accurately simulate the dynamic ocean in all details. However, such models can be useful for elucidating and exploring the mechanisms of complex systems: With certain, plausible combinations of the biogeochemical parameters, this model exhibits oscillatory solutions in which surface biogeochemical and ecosystem properties vary cyclically on annual to decadal timescales in the absence of any time dependent forcing. The timescale and amplitude of the temporal variations of TDN_{xs} in the model are not inconsistent with part of the variability observed near Hawaii. Further analysis of the model (mathematical scaling and numerical) indicates that the period of the oscillation strongly depends on the rate of exchange of mixed-layer and thermocline waters and could lie between several years and several decades for the North Pacific subtropical gyre regime, but would likely be shorter (only a year or so) in the North Atlantic.

Our study provides theoretical support for the suggestion that some part of the interannual to decadal variability of TDN_{xs}, DIN_{xs}, nitrogen fixation and ecosystem structure observed in the subtropical North Pacific and North Atlantic might be attributable to an internal, biogeochemical oscillator. Without doubt external forcing such as shifts in climate regimes are also significant and internal and external mechanisms of variability may be interwined, possibly even phase-locked. We note that this simple model does not intrinsically produce shorter timescale variability which is also observed near Hawaii, possibly driven by synoptic variability in external forcing or fine scale ocean structures not reflected at all in this idealized framework.

Over most of physical and biogeochemical parameter space explored we find completely steady solutions. Oscillatory solutions occur only in a narrow region of parameter space, suggesting at first glance that the diazotrophic oscillator is unlikely to occur in nature. However, this region is where the relative fitness of the modeled diazotrophs and other phytoplankton is closely matched. It is ecologically plausible that organisms have evolved such to enable their co-existence and maximize productivity. Perhaps this narrow region of parameter space is the ecologically relevant regime.

In addition to continued observations at the subtropical time-series sites, further theoretical studies might help to resolve such questions, with some clear candidates for next steps. While the role of iron has been much simplified in the present study, which already expresses complex dynamics, an extension of this work to include this third limiting resource should be

informative. A corresponding suite of numerical modeling studies with three-dimensional ocean circulation and biogeochemistry models including the role of iron limitation (e.g. Hood *et al.* (2004); Coles and Hood (2007)) will prove useful as well as ecological models with freer, self-assembling representations of microbial populations (Follows *et al.*, 2007). Such experiments can test the mechanistic understanding emerging from this simplified model in a more realistic setting. A suite of computationally demanding integrations will be necessary to cover the appropriate parameter space in a more realistic setting. However, current advances in computational capabilities mean that this capability is now within our reach. The relative lability and bio-availability of organic forms of N and P (Clark *et al.*, 1998; Aluwihare *et al.*, 2005) also plays a role in regulating the ecology and biogeochemistry of the oligotrophic oceans, including the possibility and nature of the oscillator. Current models, including this one, deal with this issue in an extremely simplistic way, partly reflecting the general need for greater understanding on this topic.

In summary, for the first time an idealized model has been used to support and illustrate the hypothesized internal biogeochemical oscillator in the subtropical oceans, driving cycles of nitrogen fixation and its geochemical indicators. The model provides a framework in which to explore the underlying ecology which regulates the occurrence and properties of the system. Though the biogeochemical oscillator occurs in only a small region of ecological parameter space, it is one which the relative fitness, co-existence and primary production of this simple system are optimal.

Acknowledgements. We thank Andrew Barton, Stephanie Dutkiewicz and Ariane Verdy for helpful discussion and comments. We are grateful for the work of the HOT and BATS time-series scientists which have motivated and enabled this study. We are thankful for stimulating and thoughtful comments from three anonymous reviewers. This work was supported by the National Science Foundation and the Gordon and Betty Moore Foundation Marine Microbial Initiative.

APPENDIX

Approximate solution for $d\mathrm{TDN}_{xs1}/dt$

We determine a simplified, approximate solution for the decline of the mixed layer TDN_{xs} in phases 3 and 4 (Figs. 4 and 5). The mixed layer TDN_{xs} is defined as $d\mathrm{TDN}_{xs1}/dt = dTDN_1/dt - 16dTDP_1/dt$, where the mixed layer concentrations of TDN and TDP are $TDN_1 = DIN_1 + DON_1$ and $TDP_1 = DIP_1 + DOP_1$ respectively. We assume that diazotrophs have a negligible concentration ($Dia \approx 0$) in phases 3 and 4 (see Fig. 4a) and rewrite equations for TDN_1 and TDP_1 using Eqs. (6–11) such that:

$$\frac{dTDN_1}{dt} = \frac{dDIN_1}{dt} + \frac{dDON_1}{dt}$$
$$\approx -\frac{V}{z_1}(TDN_1 - TDN2) - R^{Phy}pp + (1-S)R^{Phy}M^{Phy}Phy$$

$$\frac{dTDP_1}{dt} = \frac{dDIP_1}{dt} + \frac{dDOP_1}{dt}$$
$$\approx -\frac{V}{z_1}(TDP_1 - TDP2) - pp + (1 - S)M^{Phy}Phy$$

Because the N:P stoichiometry of non-diazotrophic phytoplankton is Redfieldian ($R^{Phy} = 16$) these two equations simplify to one for mixed layer TDN_{xs}:

$$\frac{d\mathrm{TDN}_{xs1}}{dt} \approx -\frac{V}{z_1}(\mathrm{TDN}_{xs1} - \mathrm{TDN}_{xs2}) \approx \frac{V}{z_1}\mathrm{TDN}_{xs2}$$

If the decline of the mixed layer TDN_{xs} is almost linear (see Fig. 4b, phases 3 and 4) then mixed layer TDN_{xs} is negligible relative to the thermocline TDN_{xs} ($\mathrm{TDN}_{xs1} \ll \mathrm{TDN}_{xs2}$), which is valid to first order ($\mathrm{TDN}_{xs1} \approx 0$ and $\mathrm{TDN}_{xs2} \approx -6$). Thus the decline of the mixed layer TDN_{xs} is a function only of the rate transfer of thermocline TDN_{xs} to the surface.

REFERENCES

Aluwihare, Lihini I., Daniel J. Repeta, Silvio Pantoja, and Carl G. Johnson. 2005. Two chemically distinct pools of organic nitrogen accumulate in the ocean. Science, *308*, 1007–1010.

Armstrong, R. A. and R. McGehee. 1980. Competitive exclusion. Am. Nat., *115*, 151–170.

Bates, N. R. and D. A. Hansell. 2004. Temporal variability of excess nitrate in the subtropical mode water of the North Atlantic Ocean. Mar. Chem., *84*, 225–241.

Benitez-Nelson, C. R. 2000. The biogeochemical cycling of phosphorus in marine systems. Earth-Sci. Rev., *51*, 109–135.

Berman, T. and D. Bronk. 2003. Dissolved organic nitrogen: a dynamic participant in aquatic ecosystem. Aquat. Microb. Ecol., *31*, 279–305.

Björkman, K. and D. M. Karl. 2003. Bioavailability of dissolved organic phosphorus in the euphotic zone at station ALOHA, North Pacific Subtropical Gyre. Limnol. Oceanogr., *48*, 1049–1057.

Björkman, K., A. Thomson-Bulldis, and D. M. Karl. 2000. Phosphorus dynamics in the North Pacific subtropical gyre. Aquat. Microb. Ecol., *22*, 185–198.

Boyer-Montegut, C., G. Madec, A. S. Fischer, A. Lazar, and D. Iudicone. 2004. Mixed layer depth over the global ocean: An examination of profile data and a profile-based climatology. J. Geophys. Res., *109*, C12003, doi:10.1029/2004JC002378.

Capone, D. G., J. P. Zehr, H. W. Paerl, B. Bergman, and E. J. Carpenter. 1997. *Trichodesmium*, a globally significant marine cyanobacterium. Science, *276*, 1221–1229.

Carpenter, E. J., J. P. Montoya, J. Burns, M. R. Mulholland, A. Subramaniam, and D. G. Capone. 1999. Extensive bloom of a N_2-fixing diatom/cyanobacterial association in the tropical Atlantic Ocean. Mar. Ecol. Prog. Ser., *185*, 273–283.

Carpenter, E. J. and K. Romans. 1991. Major role of the cyanobacterium *Trichodesmium* in nutrient cycling in the North Atlantic Ocean. Science, *254*, 1356–1358.

Clark, L. L., E. D. Ingall, and R. Benner. 1998. Marine phosphorus is selectively remineralized. Nature, *393*, 426.

Coles, V. J. and R. R. Hood. 2007. Modeling the impact of iron and phosphorus limitations on nitrogen fixation in the Atlantic Ocean. Biogeosciences, *4*, 455–479.

Deutsch, C., N. Gruber, R. M. Key, and J. L. Sarmiento. 2001. Denitrification and N_2 fixation in the Pacific Ocean. Global Biogeochem. Cy., *15*, 483–506.

Dugdale, R. 1967. Nutrient limitation in the sea: Dynamics, identification, and significance. Limnol. Oceanogr., *12*, 685–695.

Dutkiewicz, S., M. Follows, J. Marshall, and W. Gregg. 2001. Interannual variability of phytoplankton abundances in the North Atlantic. Dee-Sea Res. II, *45*, 2323–2344.

Falcón, Luisa I., Sybille Pluvinage, and Edward J. Carpenter. 2005. Growth kinetics of marine unicellular N_2-fixing cyanobacterial isolates in continuous culture in relation to phosphorus and temperature. Mar. Ecol. Prog. Ser., *285*, 3–9.

Fanning, Kent A. 1992. Nutrient provinces in the sea: concentration ratios, reaction rate ratios, and ideal covariation. J. Geophys. Res., *97*, 5693–5712.

Fasham, M. J. R., H. W. Ducklow and S. M. McKelvie. 1990. A nitrogen-based model of plankton dynamics in the oceanic mixed layer. J. Mar. Res., *48*, 591–639.

Fennel, K., Y. H. Spitz, R. M. Letelier, M. R. Abbott and D. M. Karl. 2002. A deterministic model for N_2 fixation at stn. ALOHA in the subtropical North Pacific Ocean. Deep-Sea Res. II, *49*, 149–174.

Follows, M. J., S. Dutkiewicz, S. Grant and S. W. Chisholm. 2007. Emergent biogeography of microbial communities in a model ocean. Science, *315*, 1843–1846.

Goebel, Nicole, Christopher A. Edwards, Brandon J. Carter, Katherine M. Achilles, and Jonathan P. Zehr. 2008. Growth and carbon content of three different-sized diazotrophic cyanobacteria observed in the subtropical North Pacific. J. Phycol., *44*, 1212–1220.

Gruber, N. 2004. The dynamics of the marine nitrogen cycle and its influence on atmospheric CO_2 variations, *in* The Ocean Carbon Cycle and Climate, M. Follows and T. Oguz, eds., 97–148.

Gruber, N. and J. L. Sarmiento. 1997. Global patterns of marine nitrogen fixation and denitrification. Global Biogeochem. Cy., *11*, 235–266.

Hansell, D. A., N. R. Bates and D. B. Olson. 2004. Excess nitrate and nitrogen fixation in the North Atlantic Ocean. Mar. Chem., *84*, 243–265.

Ho, T.-Y., A. Quigg, Z. Finkel, A. Milligan, K. Wyman, P. Falkowski and F. Morel. 2003. The elemental composition of some marine phytoplankton. J. Phycol., *39*, 1145–1159.

Hood, R. R., V. J. Coles and D. G. Capone. 2004. Modeling the distribution of *Trichodesmium* and nitrogen fixation in the Atlantic Ocean. J. Geophys. Res., *109*, C06006, doi: 10.1029/2002JC001753.

Karl, D. M. 2002. Nutrient dynamics in the deep blue sea. Trends Microbiol., *10*, 410–418.

Karl, D. M., R. Bidigare and R. Letelier. 2001. Long-term changes in plankton community structure and productivity in the North Pacific Subtropical Gyre: The domain shift hypothesis. Deep-Sea Res. II, *48*, 1449–1470.

Karl, D. M., R. Letelier, J. Dore, J. Christian and D. Hebel. 1997. The role of nitrogen fixation in biogeochemical cycling in the subtropical North Pacific Ocean. Nature, *388*, 533–538.

Karl, D. M., R. Letelier, D. Hebel, J. Dore, J. Christian, and C. Winn. 1995. Ecosystem changes in the North Pacific subtropical gyre attributed to the 1991–1992 El Niño. Nature, *373*, 230–234.

Karl, D. M., A. Michaels, B. Bergman, D. Capone, E. Carpenter, R. Letelier, F. Lipschultz, H. Paerl, D. Sigman and L. Stal. 2002. Dinitrogen fixation in the world's oceans. Biogeochemistry, *57/58*, 47–98.

Klausmeier, C., E. Litchman, T. Daufresne and S. Levin. 2004. Optimal nitrogen-to-phosphorus stoichiometry of phytoplankton. Nature, *429*, 171–174.

Landolfi, A., A. Oschlies and R. Sanders. 2008. Organic nutrients and excess nitrogen in the North Atlantic subtropical gyre. Biogeosci., *5*, 1199–1213.

Langlois, Rebecca J., Diana Hummer, and Julie LaRoche. 2008. Abundance and distributions of the dominant *nifH* phylotypes in the North Atlantic Ocean. Appl. Environ. Microb., *74*, 1922–1931.

LaRoche, J. and E. Breitbarth. 2005. Importance of the diazotrophs as a source of new nitrogen in the ocean. J. Sea Res., *53*, 67–91.

Libes, S. 1992. The production and destruction of organic compounds in the sea, *in* An Introduction to Marine Biogeochemistry, S. Libes, ed., 394–422.

Marshall, J. C., A. J. G. Nurser, and R. G. Williams. 1993. Inferring the subduction rate and period over the North Atlantic. J. Phys. Oceanogr., *23*, 1315–1329.

Masotti, I., D. Ruiz-Pino, and A. LeBouteiller. 2007. Photosynthetic characteristics of *Trichodesmium* in the southwest Pacific Ocean: importance and significance. Mar. Ecol. Prog. Ser., *338*, 47–59.

Michaels, A. F., D. Olson, J. L. Sarmiento, J. W. Ammerman, K. Fanning, R. Jahnke, A. H. Knap, F. Lipschultz and J. M. Prospero. 1996. Inputs, losses and transformations of nitrogen and phosphorus in the pelagic North Atlantic Ocean. Biogeochemistry, *35*, 181–226.

Qiu, B. and R. X. Huang. 1995. Ventilation of the North Atlantic and the North Pacific: Subduction versus obduction. J. Phys. Oceanogr., *25*, 2374–2390.

Quigg, A., Z. Finkel, A. Irwin, Y. Rosenthal, T. Ho, J. Reinfelder, O. Schofield, F. Morel, and P. Falkowski. 2003. The evolution inheritance of elemental stoichiometry in marine phytoplankton. Nature, *425*, 291–294.

Redfield, A. 1934. On the proportions of organic derivatives in seawater and their relation to the composition of plankton, *in* James Johnston memorial volume, University Press, London, 176–192.

Redfield, A., B. Ketchum and F. Richards. 1963. The influence of organisms on the composition of sea-water, *in* The Sea, vol. 2, *2*, 26–77.

Sanudo-Wilhelmy, S., A. Kustka, C. Gobler, D. Hutchins, M. Yang, K. Lwiza, J. Burns, D. Capone, J. Raven, and E. Carpenter. 2001. Phosphorus limitation of nitrogen fixation by *Trichodesmium* in the central Atlantic Ocean. Nature, *411*, 66–69.

Sohm, J. A. and D. G. Capone. 2006. Phosphorus dynamics of the tropical and subtropical North Atlantic: *Trichodesmium* spp. versus bulk plankton. Mar. Ecol. Prog. Ser., *317*, 21–28.

Steven, D. M. and R. Glombitza. 1972. Oscillatory variation of a phytoplankton population in a tropical ocean. Nature, *237*, 105–107.

Stewart, F. M. and B. R. Levin. 1973. Resource partitioning and the outcome of interspecific competition: A model and some general considerations. Amer. Natur., *107*, 171–198.

Tilman, D. 1977. Resource competition between planktonic algae: An experimental and theoretical approach, Ecology, *58*, 338–348.

Tyrrell, T. 1999. The relative influences of nitrogen and phosphorus on oceanic primary production. Nature, *400*, 525–531.

Varela, M., A. Bode, E. Fernandez, N. Gonzalez, V. Kitidis, and E. Woodward. 2005. Nitrogen uptake and dissolved organic nitrogen release in planktonic communities characterized by phytoplankton size-structure in the Central Atlantic Ocean. Deep-Sea Res. I, *52*, 1637–1661.

Williams, R. G. 2001. Ocean Subduction, *in* Encyclopedia of ocean sciences, J. H. Steele, S. A. Thorpe and K. K. Turekian, eds., Academic Press, 1982–1993.

Zehr, J. P. and B. Ward. 2002. Nitrogen cycling in the ocean: New perspectives on processes and paradigms. Appl. Environ. Microb., *68*, 1015–1024.

Zehr, J. P., J. B. Waterbury, P. J. Turner, J. P. Montoya, E. Omoregie, G. F. Stward, A. Hansen, and D. M. Karl. 2001. Unicellular cyanobacteria fix N_2 in the subtropical North Pacific Ocean. Nature, *412*, 635–638.

Received: *28 August 2008*; revised: *22 January 2009*.